Journal of Experimental Botany, Vol. 61, No. 4, pp. 1205–1213, 2010
doi:10.1093/jxb/erp391 Advance Access publication 6 January, 2010
This paper is available online free of all access charges (see http://jxb.oxfordjournals.org/open_access.html for further details)

Journal of Experimental Botany
www.jxb.oxfordjournals.org

RESEARCH PAPER

Intracellular consequences of SOS1 deficiency during salt stress

Dong-Ha Oh[1], Sang Yeol Lee[1], Ray A. Bressan[2,3], Dae-Jin Yun[1,3] and Hans J. Bohnert[3,4,*]

[1] Division of Applied Life Science (BK21 program) and Environmental BiotechnologyNational Core Research Center, Graduate School of Gyeongsang NationalUniversity, Jinju 660-701, Korea
[2] Department of Horticulture and Landscape Architecture, Purdue University, WestLafayette, IN 47907, USA
[3] WCU Program, Division of Applied Life Sciences, Gyeongsang National University, Jinju 660–701, Korea
[4] Departments of Plant Biology and of Crop Sciences, University of Illinois at UrbanaChampaign, Urbana, IL 61801, USA

* To whom correspondence should be addressed. E-mail: hbohnert@illinois.edu

Received 12 August 2009; Revised 12 December 2009; Accepted 15 December 2009

Abstract

A mutation of AtSOS1 (Salt Overly Sensitive 1), a plasma membrane Na^+/H^+-antiporter in *Arabidopsis thaliana,* leads to a salt-sensitive phenotype accompanied by the death of root cells under salt stress. Intracellular events and changes in gene expression were compared during a non-lethal salt stress between the wild type and a representative SOS1 mutant, *atsos1-1,* by confocal microscopy using ion-specific fluorophores and by quantitative RT-PCR. In addition to the higher accumulation of sodium ions, *atsos1-1* showed inhibition of endocytosis, abnormalities in vacuolar shape and function, and changes in intracellular pH compared to the wild type in root tip cells under stress. Quantitative RT-PCR revealed a dramatically faster and higher induction of root-specific Ca^{2+} transporters, including several CAXs and CNGCs, and the drastic down-regulation of genes involved in pH-homeostasis and membrane potential maintenance. Differential regulation of genes for functions in intracellular protein trafficking in *atsos1-1* was also observed. The results suggested roles of the SOS1 protein, in addition to its function as a Na^+/H^+ antiporter, whose disruption affected membrane traffic and vacuolar functions possibly by controlling pH homeostasis in root cells.

Key words: *Arabidopsis thaliana*, endocytosis, salinity tolerance, SOS1.

Introduction

Mechanisms by which plants counter salinity stress include responses that counteract the osmotic component of the stress and, typically, the exclusion of Na^+ from tissues. A major mechanism leading to tissue tolerance engages cellular adjustments that sequester Na^+ into vacuoles (Munns and Tester, 2008). SOS1, a plasma membrane Na^+/H^+-antiporter, is an important tolerance determinant, involved in the exclusion of sodium ions from cells (Shi *et al.*, 2000, 2002). This antiporter forms one component in a mechanism based on sensing of the salt stress that involves increases of cytosolic $[Ca^{2+}]$, protein interactions and reversible phosphorylation with SOS1 acting in concert with SOS2 and SOS3 (Guo *et al.*, 2004; Halfter *et al.*, 2000; Quintero *et al.*, 2002). Compartmentalization of Na^+ that escapes export into vacuoles through SOS1 action is considered to be mediated by NHX1, a vacuolar membrane Na^+/H^+-antiporter (Apse *et al.*, 1999, 2003). Overexpression of AVP1, a vacuolar H^+-pyrophosphatase (H^+-PPase) resulted in improved salt-tolerance with higher vacuolar sodium accumulation, indicating the critical importance of pH homeostasis on Na^+ sequestration and tissue tolerance (Gaxiola *et al.*, 2001; Munns and Tester, 2008).

During the initial phase of salt stress, cell level tolerance appears critical especially for root cells, as early sodium influx is connected to the transpirational pull of water (Läuchli *et al.*, 2008). The severe salt sensitivity of *sos1* mutants at the early stages of stress suggested a function in protecting root cells, which was recognizable by the high

expression of *SOS1* in the root tip epidermis (Shi *et al.*, 2002). This function is typically associated with the Na^+/H^+ antiporter nature of the SOS1 protein, essentially the export of Na^+ ions that have entered the cytosol. In this function, SOS1 is part of a complex of transporters, and, considering the extreme salt sensitivity of *sos1* mutants, possibly the weakest link in a chain. Tissue tolerance then involves the maintenance of intracellular ion homeostasis, achieved by a dynamic network of ion transporters and related proteins that are viewed as regulated by changes in intracellular pH and $[Ca^{2+}]$ in a highly saline environment (Chinnusamy *et al.*, 2006). Deletion of *SOS1* affects proton-flux in the *Arabidopsis* root, suggesting an involvement in pH homeostasis (Shabala *et al.*, 2005). Generally, changes in the proton gradient and cytoplasmic pH will affect cellular processes such as pH-responsive activities of vacuolar Ca^{2+}/H^+ transporters (CAX1 and CAX2) (Pittman *et al.*, 2005). Increased cytosolic $[Ca^{2+}]$ would activate calcium-binding proteins, including SOS3, which binds and activates the protein kinase SOS2 (Halfter *et al.*, 2000). The activated SOS2/3 complex, in turn, can activate CAX1 (Cheng *et al.*, 2004), NHX1 or other transporters involved in vacuolar Na^+ transport (Qiu *et al.*, 2004), and SOS1 itself (Qiu *et al.*, 2002). Export of Na^+, for example, by an Na^+/H^+ antiporter will change the cytosolic and the vacuolar pH (Leshem *et al.*, 2006). In a different pH- and $[Ca^{2+}]$-dependent pathway, vacuolar Na^+/H^+ transport activity and the selectivity of NHX1 are regulated by the calmodulin-like CaM15 (Yamaguchi *et al.*, 2005). AVP1 is not only involved in Na^+-compartmentalization into vacuoles, but is also critical for maintaining endocytosis and auxin transport (Li *et al.*, 2005), implying that maintenance of vacuolar pH under salt stress should be critical for continued growth and, in turn, generating more cells and vacuoles that are then able to sequester sodium (Hasegawa *et al.*, 2000).

Despite the accumulating evidence of SOS1 involvement in cellular ion homeostasis, little attention has been paid on functions other than Na^+ exclusion at the whole plant level. There have been limited studies targeting the SOS1 regulation of gene expression (Gong *et al.*, 2001; Oh *et al.*, 2007), and only a few attempts to describe the strong salt sensitivity at the cellular level upon SOS1 deletion by integrating pH, $[Ca^{2+}]$, and other cellular events. In a previous study, it has been shown that an RNAi-based decreased expression of the *SOS1* orthologue in *Thellungiella halophila*, a halophytic relative of *Arabidopsis*, resulted in the premature death of root cells in the meristem and the elongation zone. This then allowed the unchecked apoplastic flux of sodium ions into the stele and into the shoot, leading to salt sensitivity and the loss of halophytism at the whole plant level (Oh *et al.*, 2009). Here, we describe cellular events of an *Arabidopsis SOS1* knockout mutant, *sos1-1* (Shi *et al.*, 2002) in root cells under salt stress using different ionophores and the fluorescent membrane probe FM4-64. Analysing the expression pattern of ion (including proton) transporters and vesicle trafficking-related genes, the observations have been reconciled with the complex genetic structure of transport entities that have emerged in recent years. The results highlight the critical roles of SOS1, which appear to go significantly beyond its Na^+/H^+ antiporter activity, in supporting vacuolar morphology, ion homeostasis, and membrane trafficking, subsequently mediating the tissue tolerance of root cells during the early stages of salt stress.

Materials and methods

Plant material and stress treatment

Seedlings were germinated and grown on quarter-strength MS (Murashige-Skoog) media supplemented with 0.5% MES buffer (pH 5.8), 2% sucrose, and 0.7% Select-Agar (Invitrogen). Five-day-old seedlings were transferred to vertical agar plates supplemented with 100 mM NaCl for the indicated time. For confocal microscopy, at least 10 seedlings were analysed and representative images are shown. Twenty seedlings were pooled for expression analyses.

Confocal microscopy

Following treatment, seedlings were incubated with fluorescent dyes in liquid media of the same composition used in the stress treatment. For the visualization of sodium, seedlings were incubated with 5 μM CoroNa Green-AM (Invitrogen) for 2 h. Where confocal planes of the centre plane were required, seedlings were incubated for 8 h on a filter paper soaked with media supplemented with 2.5 μM CoroNa Green-AM, before washing and confocal microscopy at excitation and emission wavelengths of 488 nm and 516 nm, respectively, as described by Oh *et al.* (2009). Negative control pictures of roots incubated without Na^+ ions are presented in Supplementary Fig. S3 at *JXB* online. For analyses of intracellular pH, 10 μM carboxyl SNARF-AM (Invitrogen) was applied in the presence of 0.01% pluronic acid (Invitrogen) for 2 h. The ratio of average fluorescence intensities collected from the acidic (570–590 nm) and basic (630–650 nm) components with a single excitation wavelength at 488 nm were analysed by ImageJ software (NCBI). pH values were calculated by *in situ* calibration (see Supplementary Fig. S4 at *JXB* online) as described by the supplier (Invitrogen, MP01270). To visualize calcium, 20 μM Fluo4-AM was loaded in the presence of pluronic acid for 2 h. In separate experiments, Calcein-AM (Invitrogen), a non-ion specific fluorescence dye with similar molecular weight,was substituted for Fluo4-AM to ensure the same efficiency of dye loading between Col3 and *sos1-1* root cells. Excitation and emission wavelengths of 488 nm and 516 nm were used for both Fluo4 and Calcein dyes. Where indicated, 1 μg ml^{-1} propidium iodide (Invitrogen) was added to counterstain the cell wall and dead cells. To visualize membrane trafficking, 5 μM FM4-64 (Invitrogen) was loaded for 5 min and the seedlings were incubated for a further 30 min after the removal of FM4-64.

Expression analysis

Roots from 20 seedlings were pooled and gene expression was analysed by qPCR as described by Gong *et al.* (2005). The primers are listed in Supplementary Table S2 at *JXB* online. Experiments were repeated six times (two biological and three analytical repeats).

Results

Sodium accumulation and membrane trafficking under salt stress

Sodium ions were visualized using a sodium-specific fluorescent dye, CoroNa Green (Invitrogen). After 8 h in 100 mM

NaCl, no significant differences in fluorescence intensity were observed between cells of Col3 and *sos1-1* in the root meristem and cell elongation regions. By contrast, differences appeared in the shape of the vacuoles and the internalization of FM4-64 (Invitrogen) used to counterstain membranes (Fig. 1). While the shape of the vacuoles was not affected by NaCl in Col3 cells (Fig. 1A), root cells of *sos1-1* showed shrunken central vacuoles of globular shape (Fig. 1B). The internalization of FM4-64 was normal under non-stress conditions (Fig. 1C, E), but inhibited only in *sos1-1* root meristematic cells under salt stress (Fig. 1D, F). After prolonged stress, differences in CoroNa Green intensity became pronounced, with higher fluorescence in the root tip region of *sos1-1* than in Col3 (Fig. 2A, B). While the Col3 roots remained intact, cell death was observed in the root tip region of sos1 after 20 h (Fig. 2C, D). Cell death started about 14 h into the stress treatment in older parts of roots of *sos1-1*. Root cells of Col3 contained CoroNa Green fluorescence exclusively in the vacuoles, and propidium iodide stained the cell wall (Fig. 2E, G). In *sos1-1* roots, the cell interior increasingly became stained by propidium iodide (Fig. 2F, arrow), and adjacent cells showed leakage of sodium-specific fluorescence out of the vacuoles (Fig. 2H, arrow). Optical dissections at the centre plane of the older part of the roots (Fig. 2I, J) revealed sodium-specific fluorescence confined to the epidermis (Ep) and cortex (Co) layers, while no fluorescence was observed in the stele (St) in Col3 roots (Fig. 2I). By contrast, *sos1-1* roots showed cortex cells with fragmented, globule-shaped vacuoles and significant fluorescence in the stele (Fig. 2J).

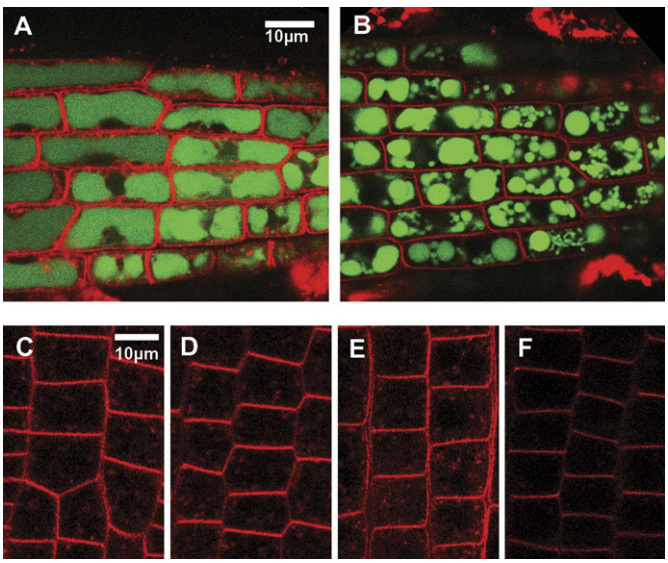

Fig. 1. Visualization of sodium and endocytosis. (A, B) Confocal planes showing young cortex cells at the root tip region of Col3 (A) or *sos1-1* (B) after a 8 h treatment with 100 mM NaCl. Seedlings were stained with CoroNa Green (green) and FM4-64 (red). (C–F) Cells at the root meristem of Col3 (C, D) or *sos1-1* (E, F) under non-stress condition (C, E) or after 8 h treated with 100 mM NaCl (D, F). Shown were pictures taken at 30 min after application of FM4-64 at the same confocal setting.

Intracellular pH and calcium

Carboxyl-SNARF (Invitrogen) was used to visualize the intracellular pH in the root tip region (Fig. 3). Without stress, Col3 and *sos1-1* roots showed no differences (Fig. 3A, B). After 8 h in 100 mM NaCl, the vacuole of Col3 became more alkaline, indicated by a fluorescence red-shift

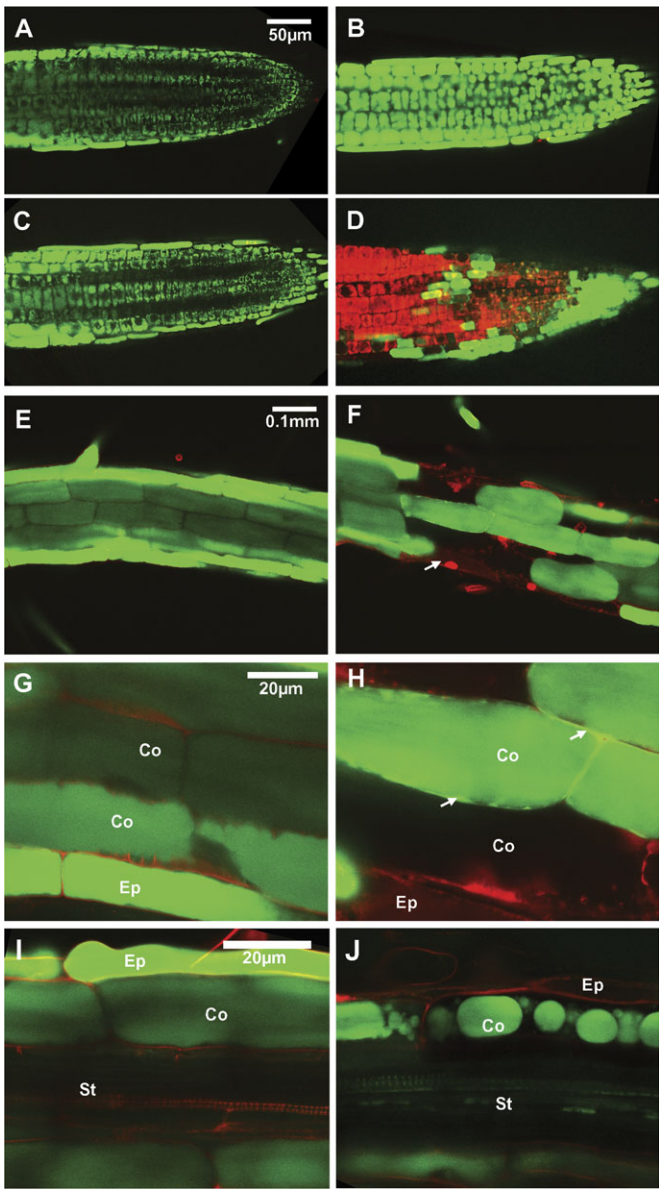

Fig. 2. Effects of long-term stress. CoroNa Green (green) was applied to visualize sodium and propidium iodide (red) to stain the cell wall and dead cells. (A–D) Root tip region after 14 h (A, B) and 20 h (C, D) treatment with 100 mM NaCl. Confocal planes showing epidermis and cortex cells of the Col3 (A, C) or *sos1-1* (B, D). (E–F) Root hair zone of Col3 (E) and *sos1-1* (F) after 14 h treatment with 100 mM NaCl. Confocal planes showing epidermis (Ep) and cortex (Co) cells. (G) Magnification of images in (E). (H) Magnification of images in (F). (I, J) Older parts of Col3 (G) and *sos1-1*(H) roots after 20 h treatment with 100 mM NaCl. Confocal planes showing epidermis (Ep), cortex (Co) layers, and stele (St).

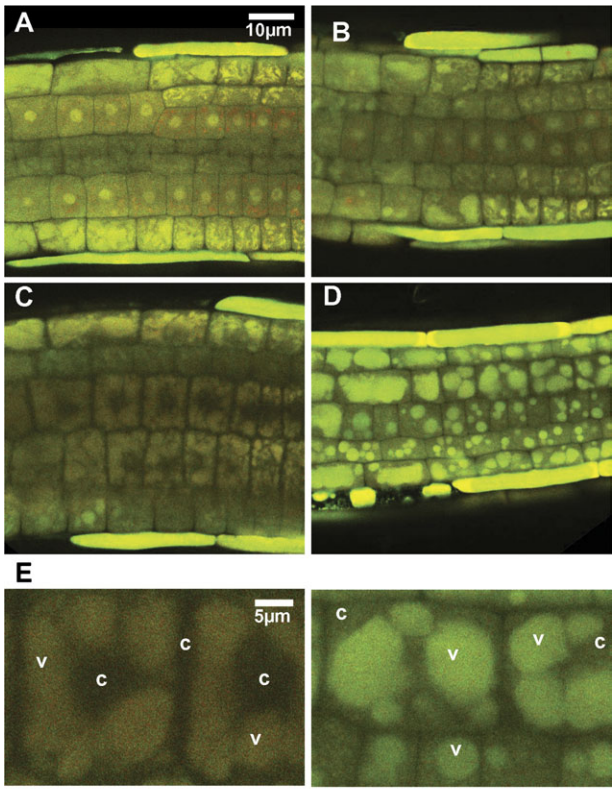

	Vacuole	Cytosol
Col3	7.82 ± 0.05	7.71 ± 0.14
sos1-1	7.26 ± 0.04	7.42 ± 0.10

Fig. 3. Changes in intracellular pH under salt stress. (A–D) Carboxyl SNARF-AM, which shifts the emission wavelength to red at higher pH, was applied to visualize the intracellular pH. Confocal planes collected from GFP and RFP channel were superimposed. Epidermis and cortex cells at the root tip region of Col3 (A, C) or *sos1-1* (B, D) under non-stress condition (A, B) or after 8 h treatment with 100 mM NaCl (C, D). (E) Analyses of pH at the cytosol (c) or vacuole (v) from cells of (C) and (D). The pH values were deduced from the ratio of RFP and GFP channel intensities as described in the Materials and methods section; also see Supplementary Fig. S4 at *JXB* online.

(Fig. 3C), while the shrunken vacuoles of the *sos1-1* root cells showed green-shift (Fig. 3D), indicating acidification. The ratios of red/green in the fluorescence channel of cytosol (c) and vacuole (v) were measured and the intracellular pH values were calculated as described in the Materials and methods section (Fig. 3E; see Supplementary Fig. S4 at *JXB* online). The deduced average pH values of the cytoplasm and the vacuole were 7.71 and 7.82, respectively, for Col3, and 7.42 and 7.26 for *sos1-1*. Calcium was visualized using Fluo4-AM (Invitrogen). In the absence of stress, *sos1-1* did not show significant differences compared to Col3 (Fig. 4A, B). After a 2 h treatment at 100 mM NaCl, both the wild type and *sos1-1* showed vacuole-located fluorescence at significantly higher intensity in the *sos1-1* root cells (Fig. 4C, D).

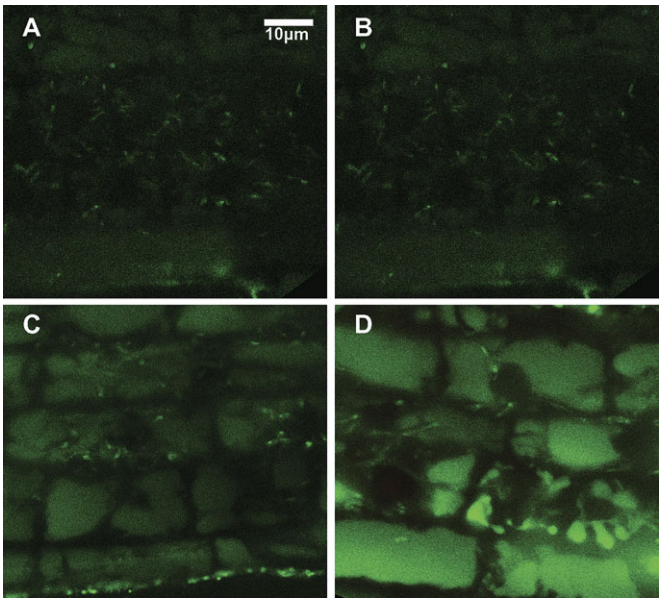

Fig. 4. Visualization of calcium after salt stress. Fluo-4 was used for staining calcium in the root cells without stress (A, B) or after 2 h treatment of 100 mM NaCl (C, D). Shown are the cortex cells at the elongation zone of Col3 (A, C) and *sos1-1* (B, D).

Expression of genes related to pH homeostasis and membrane trafficking

To characterize the genetic basis of the observations on vacuolar morphology, membrane trafficking, and pH homeostasis, the expression patterns were compared between Col3 and *sos1-1* roots by qPCR for selected genes, including genes involved in pH homeostasis, membrane traffic-related proteins, and aquaporins (Fig. 5; see Supplementary Table S1 at *JXB* online). A cytochrome *c*1 precursor gene (At5g40810) was selected as a reference transcript, based on the uniformity of expression in the root under abiotic stresses (Czechowski *et al.*, 2005). Treatment with 100 mM NaCl for 2 h was added to analyse the early responses together with the 8 h time point used for most of the microscopic studies. Among the pH-related transporters, AHA1 and AHA2, encoding plasma membrane proton ATPases, AVA-P4, a vacuolar proton ATPase, and AVP1, a vacuolar H^+-PPase, were significantly down-regulated in *sos1-1* after 8 h compared to the wild type (Fig. 5A; see Supplementary Table S1 at *JXB* online). An analysis of clusters of orthologous groups of proteins encoded in the *Arabidopsis* genome (http://www.ncbi.nlm.nih.gov/COG/) revealed more than 500 genes involved in membrane trafficking. Among these, several genes encoding exocyst subunits and syntaxins were highly regulated in a previous transcriptome analysis of a *Thellungiella* line expressing *ThSOS1*-RNAi (*thsos1-4*) (Oh *et al.*, 2007). At least two exocyst subunit genes, EXO70B1 and EXO70H7, and two syntaxins, SYP121 and SYP122, were induced in the *Arabidopsis sos1-1* line, while SYP111/KNOLE and an ARF-GEF, GNOM, were down-regulated specifically in *sos1-1* after 8 h. The gene of a clathrin adaptor subunit,

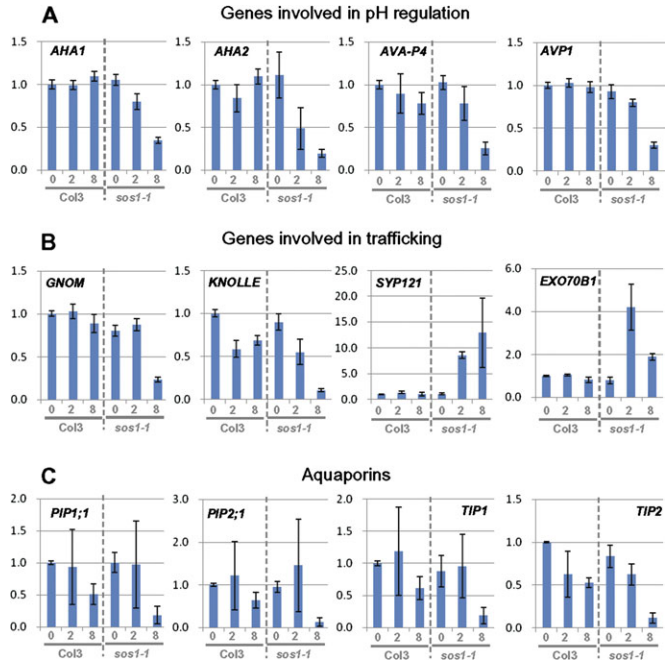

Fig. 5. Expression pattern of genes encoding pH, membrane trafficking-related proteins, and aquaporins. Gene expression was compared by qPCR between roots of Col3 and *sos1-1* after 0, 2, and 8 h treatment with 100 mM NaCl. Shown are fold changes compared to the Col3 under non-stress condition. Error bars indicate standard deviations from six repeats (two biological×three analytical). Selected genes encoding pH (A), membrane trafficking-related proteins (B) and aquaporins (C). For the complete list of analyses, see Supplementary Table S1 at *JXB* online.

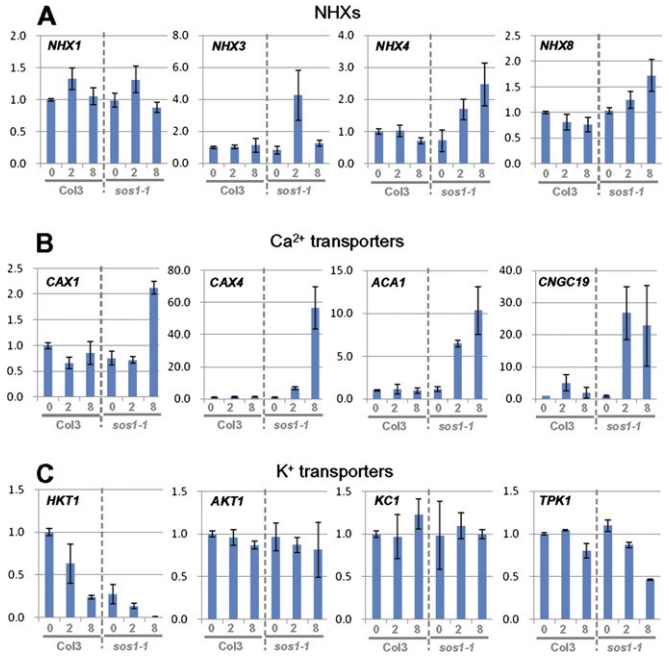

Fig. 6. Expression pattern of genes encoding ion transporters. Selected genes of NHX family (A), Ca^{2+} transporters (B) and K^+ transporters. For the complete list of analyses, see Supplementary Table S1 at *JXB* online.

coatomer zeta-1, was greatly induced in *sos1-1*, especially at longer stress treatments (Fig. 5B; see Supplementary Table S1at *JXB* online). Aquaporins, both in the plasma membrane and tonoplast sub-families, were down-regulated after 8 h in both Col3 and *sos1-1*, with a greater decrease found in *sos1-1* roots (Fig. 5C; see Supplementary Table S1 at *JXB* online).

Expression of ion transporters

The expression of all NHX family genes, apart from SOS1, being inactivated by a frame-shift mutation in *sos1-1*, have been examined. NHX1 and NHX2, the two most abundantly transcribed genes of the family, both known as vacuolar membrane proteins, showed no significant differences in expression between Col3 and *sos1-1*. Expression of the less abundant NHX5 and NHX6 were equally unaffected, while NHX3, NHX4 and NHX8 were induced significantly in *sos1-1* (Fig. 6A; see Supplementary Fig. S1 at *JXB* online). By contrast, HKT1 expression decreased in both Col3 and *sos1-1* under salt stress, with a much stronger decrease in *sos1-1* to nearly undetectable mRNA levels by 8 h of salt stress (Fig. 6C; see Supplementary Table S1 at *JXB* online). In a previous study on *Thellungiella* SOS1, several Ca^{2+} transporters and related genes, i.e. CAX4, ACA1, and 5PTase2, were among the most highly induced genes following the reduction of ThSOS1 under salt stress (Oh *et al.*, 2007). In *Arabidopsis*, CAX1 and CAX2, the two most abundantly transcribed members of the CAX family, showed induction only in *sos1-1* after 8 h. Most dramatic was the induction of CAX4 by a more than 50-fold increase after 8 h in *sos1-1* roots, while CAX4 was induced only 1.3-fold in Col3. ACA1, 5PTase2, and two cyclic-nucleotide gated channels, CNGC19 and CNGC14, the most abundantly expressed genes in their family in roots, showed similar up-regulation specific for *sos1-1*. Remarkably, CNGC19 was induced 30-fold in *sos1-1* at 2 h, while it was up-regulated 5-fold and later declined in Col3 (Fig. 6B; see Supplementary Table S1 at *JXB* online). Among the potassium transporters, HKT1 showed the greatest difference. It was significantly down-regulated by salt stress in the Col3 and down-regulated by an even higher magnitude in *sos1-1*. TPK1 also showed a larger decrease in *sos1-1* compared to Col3, while AKT1 and KC1 did not show significant differences between Col3 and *sos1-1* (Fig. 6C; see Supplementary Table S1 at *JXB* online).

Discussion

The salt-sensitive phenotype of *sos1* mutants has been well documented (Wu *et al.*, 1996; Shi *et al.*, 2000, 2002), but the impact of this mutation on the level of cellular structure or on gene expression in the most affected cells has received less attention. The responses to salt stress in *Arabidopsis* wild type and *sos1-1* root cells were compared here. Based

on the function of SOS1 as a sodium extruder from cells in which it is expressed, it was expected that cellular events and gene expression patterns in *sos1-1* roots would mirror a magnification of events that have often been observed in wild-type plants under salt stress. However, not only was a much more pronounced salt stress response than in the wild type observed, but there were at least three distinct cellular events that were specific to the *sos1-1* mutant plants, suggesting additional, other than sodium/proton antiport, roles for SOS1.

Disrupted vacuolar functions in sos1-1 *root cells under salt stress*

An early and conspicuous difference between Col3 and *sos1-1* root cells under salt stress concerned the morphology of the central vacuoles (Fig. 1A, B). Differences in CoroNa Green fluorescence intensity of the vacuoles was observed after prolonged stress (Fig. 2A, B), accompanying cell death in the *sos1-1* root cells (Fig. 2D, F). Earlier, shrinkage of vacuoles had started in *sos1-1* root cells (Figs 1B, 2J), resembling the observed loss of turgor and water potential in the vacuole (Kutsuna and Hasezawa, 2005), suggesting that *sos1-1* root cells suffer a stress based on the disruption of the water potential equilibrium, even before the higher accumulation of sodium due to the lack of extrusion became significant. Consistent with this observation is a dramatic down-regulation of the expression of plasma membrane and tonoplast aquaporins only in *sos1-1* within 8 h (Fig. 6C; see Supplementary Table S1 at *JXB* online). Prolonged stress also resulted in the failure of vacuolar sodium confinement only in *sos1-1* root cells (Fig. 2H). The leakage of CoroNa Green fluorescence from vacuoles was mainly observed in cells adjacent to damaged cells which became permeable to propidium iodide, suggesting vacuolar disintegration as a last step in *sos1-1* root cells preceding cell death. To address the question whether the observations on *sos1-1* root cells resulted from a higher accumulation of Na^+ due to the absence of a Na^+ excluder function, the wild-type Col3 root cells were treated with a higher concentration of NaCl. After 12 h treatment with 200 mM NaCl, the older part of the wild-type root exhibited cell damage (arrows in Supplementary Fig. S1, at *JXB* online) and CoroNa Green fluorescence intensities were comparable with or even higher than those found in *sos1-1* root cells in Fig. 2B. However, the vacuoles of Col3 root cells maintained normal morphology, suggesting that the vacuolar deformation observed in *sos1-1* root cells is not a result of higher intracellular Na^+ accumulation (see Supplementary Fig. S1 at *JXB* online).

Inhibition of membrane trafficking in sos1-1 *under salt stress*

Another difference between Col3 and *sos1-1* root cells at the earlier stages of salt stress was observed by counterstaining the membranes with FM4-64. Both inclusion and intensity of membrane staining of FM4-64 decreased in *sos1-1* after 8 h of stress (Fig. 1C–F). A possible explanation can be found in the reports of pH and salinity-dependent changes in lipid and sterol composition in fungal species (Turk *et al.*, 2004, 2007). The observed inhibition of membrane trafficking was also reflected in the down-regulation of transcripts for GNOM and KNOLLE in the *sos1-1* root cells (Fig. 5B), indicating the inhibition of trafficking, auxin transport (Kleine-Vehn *et al.*, 2008) and cell division (Reichardt *et al.*, 2007). By contrast, SYP121 and SYP122, which are SNAREs specifically involved in the secretory pathway to the plasma membrane (Tyrrell *et al.*, 2007), were dramatically induced only in *sos1-1* roots. There was also the induction of transcripts of at least two members of the exocyst family, EXO70B1 and EXO70H7 (Hala *et al.*, 2008), suggesting an activation of a secretory or an exocytosis pathway in the *sos1-1* root cells under salt stress.

Changes of vacuolar pH in wild type and sos1-1 *under salt stress*

Ion accumulation and expression of ion transporters in *sos1-1* generally mirrored a more severe salt stress than the wild type. Removal of the SOS1 extruder function resulted in higher sodium ion accumulation in the *sos1-1* vacuole after prolonged stress (Fig. 2A, B). SOS1 mutations led to more severe potassium deficiency than that experienced by the wild type under the same stress conditions (Wu *et al.*, 1996), which might be explained by a more drastic decline of HKT1 (Rus *et al.*, 2001, 2004) and TPK1 (Gobert *et al.*, 2007) expression and/or activity in *sos1-1* under salt stress (Fig. 6C). Salt stress leads to an increase in free intracellular Ca^{2+} mainly in root cells (Tracy *et al.*, 2008). The accumulation of vacuolar free Ca^{2+} and transcripts of Ca^{2+} transporters were significantly higher in *sos1-1* (Figs 4, 6B), suggesting increased and chronic stress signalling in *sos1-1* root cells, which then experienced an amplified version of salt stress. Changes in vacuolar pH were fundamentally different in *sos1-1* cells compared to the wild type under salt stress. In another study using salt-tolerant quince protoplasts, adding NaCl higher than 100 mM to the media increased the cytosolic pH (D'Onofrio and Lindberg, 2009). A study using the *Arabidopsis* wild type showed significant increases in vacuolar pH after incubation in 200 mM NaCl for 18 h (Leshem *et al.*, 2006). The accumulation of sodium to the vacuole *via* Na^+/H^+ antiporters of the NHX-type is expected to result in the vacuoles becoming more alkalinized than the cytoplasm (Fig. 3C, E; see Supplementary Fig. S2 at *JXB* online). However, *sos1-1* cells showed more acidic vacuoles than their cytoplasm (Fig. 3D, E), although *sos1-1* plants showed a higher accumulation of sodium in their vacuoles (Fig. 2A, B). The unexpected result seems to indicate the involvement of SOS1 in a function other than the anticipated function of a Na^+/H^+ antiporter in pH homeostasis. Significantly, members of genes involved in pH regulation at both plasma membranes and tonoplasts (Martinoia *et al.*, 2007) were down-regulated only in *sos1-1* root cells (Fig. 5A).

Novel functions of SOS1 other than sodium exclusion

The distinct cellular events in *sos1-1* root cells under salt stress are summarized in juxtaposition with wild-type cells (Fig. 7). The removal of Na^+ from the cytoplasm into the extracellular space is the expected SOS1 function (Fig. 7A), but the lack of SOS1 also affects the confinement of Na^+ into vacuoles, supporting the previously stated regulatory influence of the SOS pathway on at least some vacuolar ion transporters (Cheng *et al.*, 2004; Qiu *et al.*, 2004). In wild-type root cells, the vacuoles became more alkaline (Leshem *et al.*, 2006), but this was not observed in the mutant. In *sos1-1* plants (Fig. 7B), the initial loss of vacuolar turgor and functioning, followed by excessive sodium ion entry into the vacuoles and the inhibition of membrane trafficking, resulted in membrane defects and death of root cells. Consequently, Na^+ flux into the transpiration stream increased *via* an apoplastic pathway. Disruption of vacuolar pH and down-regulation of AVP1 (Fig. 7B, red circle) might be at the core of the observations. Inhibition of AVP1 expression will affect endocytosis and auxin transport (Li *et al.*, 2005) as well as the vacuolar sequestration of sodium ion (Gaxiola *et al.*, 2001) in *sos1-1* cells under salt stress (Fig. 7B, a). Acidic vacuoles affect the activity of NHX1 by enhancing the binding of an inhibitory regulator, AtCaM15, to the luminal c-terminus (Yamaguchi *et al.*, 2005), partially explaining the failure of vacuolar sodium sequestration after prolonged stress (Fig. 7B, b).

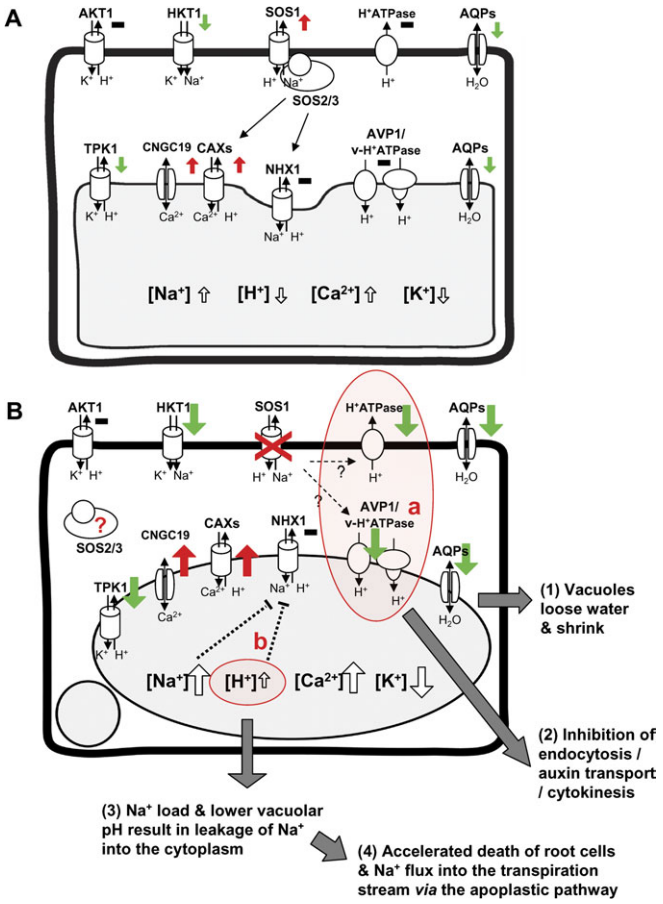

Fig. 7. Consequences of SOS1 mutation in the root cell. A diagram summarizing cellular events of wild-type (A) and *sos1-1* (B) root cells under salt stress. The coloured arrows indicated the transcriptional regulation of ion transporters, red; induction, black; no change, green; inhibition of gene expression. The size of the arrows depicts the magnitude of regulation comparing wild type and *sos1-1*.

An effect of SOS1 on the regulation of proton flux in the root tip (Shabala *et al.*, 2005) notwithstanding, our results add another dimension. The mechanism(s) by which the SOS pathway is at the basis of salt tolerance (Zhu, 2001), and how SOS1 determines halophytism (Oh *et al.*, 2009) also seem to include the mediation of vacuolar functions and pH homeostasis. In essence, the SOS pathway, and SOS1 in particular, appear to be more complex than expected. The involvement of a plasma membrane Na^+/H^+-antiporter in pH homeostasis has been documented in animals. The NHE protein family consists of nine antiporters with long C-terminal cytoplasmic tails (Orlowski and Grinstein, 2007), comparable to the plant NHX family of ight members, including SOS1 and NHX1. The C-terminal of the animal NHE1 acts as a scaffold for the assembly of a signalling complex (Baumgartner *et al.*, 2004) and NHE3 travels along the plasma membrane and endosomes, regulating endosomal pH and trafficking (Orlowski and Grinstein, 2007). Among the plant proteins, only SOS1 includes a C-terminal extension comparable to the animal proteins. The C-terminal tail of SOS1 appears to interact with a regulatory protein, RCD1, involved in oxidative stress (Katiyar-Agarwal *et al.*, 2006), but detailed studies on *in vivo* interacting partners are still lacking. The distinct cellular events observed in *sos1-1* mutant plants identify as yet unknown functions of SOS1 in mediating vacuolar integrity, membrane trafficking, and pH homeostasis under salt stress, suggesting a more dynamic role of the SOS1 protein in which the Na^+/H^+ antiporter describes only one function.

Supplementary data

Supplementary data can be found at *JXB* online.

Supplementary Fig. S1. *Col3* root at higher sodium concentration.

Supplementary Fig. S2. Intracellular pH of *Col3* root cells under higher sodium concentration.

Supplementary Fig. S3. CoroNa Green negative controls.

Supplementary Fig. S4. Determination of pH with carboxy SNARF pH indicator.

Supplementary Table S1. Complete list of qRT-PCR results.

Supplementary Table S2. List of qRT-PCR primers.

Acknowledgements

The work has been supported by the World Class University Program (grant no. R32–10148), the Environmental

Biotechnology National Core Research Center Project (grant no. R15-2003-012-01002-00) and the Biogreen 21 project of the Rural Development Administration (grant no. 20070301034030) from Korea, and institutional funds from UIUC and Purdue University.

References

Apse MP, Aharon GS, Snedden WA, Blumwald E. 1999. Salt tolerance conferred by overexpression of a vacuolar Na^+/H^+antiport in Arabidopsis. *Science* **285,** 1256–1258.

Apse MP, Sottosanto JB, Blumwald E. 2003. Vacuolar cation/H^+exchange, ion homeostasis, and leaf development are altered in a T-DNA insertional mutant of AtNHX1, the Arabidopsis vacuolar Na^+/H^+ antiporter. *The Plant Journal* **36,** 229–239.

Baumgartner M, Patel H, Barber DL. 2004. Na^+/H^+exchanger NHE1 as plasma membrane scaffold in the assembly of signaling complexes. *American Journal of Physiology–Cell Physiology* **287,** C844–C850.

Cheng NH, Pittman JK, Zhu JK, Hirschi KD. 2004. The protein kinase SOS2 activates the Arabidopsis H^+/Ca^{2+}antiporter CAX1 to integrate calcium transport and salt tolerance. *Journal of Biological Chemistry* **279,** 2922–2926.

Chinnusamy V, Zhu J, Zhu JK. 2006. Salt stress signaling and mechanisms of plant salt tolerance. *Genetic Engineering* **27,** 141–177.

Czechowski T, Stitt M, Altmann T, Udvardi MK, Scheible WR. 2005. Genome-wide identification and testing of superior reference genes for transcript normalization in Arabidopsis. *Plant Physiology* **139,** 5–17.

D'Onofrio C, Lindberg S. 2009. Sodium induces simultaneous changes in cytosolic calcium and pH in salt-tolerant quince protoplasts. *Journal of Plant Physiology* **166,** 1755–1763.

Gaxiola RA, Li J, Undurraga S, Dang LM, Allen GJ, Alper SL, Fink GR. 2001. Drought- and salt-tolerant plants result from overexpression of the AVP1 H^+-pump. *Proceedings of the National Academy of Sciences, USA* **98,** 11444–11449.

Gobert A, Isayenkov S, Voelker C, Czempinski K, Maathuis FJ. 2007. The two-pore channel TPK1 gene encodes the vacuolar K^+ conductance and plays a role in K^+ homeostasis. *Proceedings of the National Academy of Sciences, USA* **104,** 10726–10731.

Gong Q, Li P, Ma S, Indu Rupassara S, Bohnert HJ. 2005. Salinity stress adaptation competence in the extremophile *Thellungiella halophila* in comparison with its relative *Arabidopsis thaliana*. *The Plant Journal* **44,** 826–839.

Gong Z, Koiwa H, Cushman MA, *et al*. 2001. Genes that are uniquely stress regulated in salt overly sensitive (*sos*) mutants. *Plant Physiology* **126,** 363–375.

Guo Y, Qiu QS, Quintero FJ, Pardo JM, Ohta M, Zhang C, Schumaker KS, Zhu JK. 2004. Transgenic evaluation of activated mutant alleles of SOS2 reveals a critical requirement for its kinase activity and C-terminal regulatory domain for salt tolerance in *Arabidopsis thaliana*. *The Plant Cell* **16,** 435–449.

Hala M, Cole R, Synek L, *et al*. 2008. An exocyst complex functions in plant cell growth in Arabidopsis and tobacco. *The Plant Cell* **20,** 1330–1345.

Halfter U, Ishitani M, Zhu JK. 2000. The Arabidopsis SOS2 protein kinase physically interacts with and is activated by the calcium-binding protein SOS3. *Proceedings of the National Academy of Sciences, USA* **97,** 3735–3740.

Hasegawa PM, Bressan RA, Zhu JK, Bohnert HJ. 2000. Plant cellular and molecular responses to high salinity. *Annual Review of Plant Physiology and Plant Molecular Biology* **51,** 463–499.

Katiyar-Agarwal S, Zhu J, Kim K, Agarwal M, Fu X, Huang A, Zhu JK. 2006. The plasma membrane Na^+/H^+ antiporter SOS1 interacts with RCD1 and functions in oxidative stress tolerance in Arabidopsis. *Proceedings of the National Academy of Sciences, USA* **103,** 18816–18821.

Kleine-Vehn J, Dhonukshe P, Sauer M, Brewer PB, Wisniewska J, Paciorek T, Benkova E, Friml J. 2008. ARF GEF-dependent transcytosis and polar delivery of PIN auxin carriers in Arabidopsis. *Current Biology* **18,** 526–531.

Kutsuna N, Hasezawa S. 2005. Morphometrical study of plant vacuolar dynamics in single cells using three-dimensional reconstruction from optical sections. *Microscopy Research and Technique* **68,** 296–306.

Läuchli A, James RA, Huang CX, McCully M, Munns R. 2008. Cell-specific localization of Na^+ in roots of durum wheat and possible control points for salt exclusion. *Plant, Cell and Environment* **31,** 1565–1574.

Leshem Y, Melamed-Book N, Cagnac O, Ronen G, Nishri Y, Solomon M, Cohen G, Levine A. 2006. Suppression of Arabidopsis vesicle-SNARE expression inhibited fusion of H_2O_2-containing vesicles with tonoplast and increased salt tolerance. *Proceedings of the National Academy of Sciences, USA* **103,** 18008–18013.

Li J, Yang H, Peer WA, *et al*. 2005. Arabidopsis H^+-PPase AVP1 regulates auxin-mediated organ development. *Science* **310,** 121–125.

Martinoia E, Maeshima M, Neuhaus HE. 2007. Vacuolar transporters and their essential role in plant metabolism. *Journal of Experimental Botany* **58,** 83–102.

Munns R, Tester M. 2008. Mechanisms of salinity tolerance. *Annual Review of Plant Biology* **59,** 651–681.

Oh DH, Gong Q, Ulanov A, Zhang Q, Li Y, Ma W, Yun DJ, Bressan RA, Bohnert HJ. 2007. Sodium stress in the halophyte *Thellungiella halophila* and transcriptional changes in a *thsos1*-RNA interference line. *Journal of Integrative Plant Biology* **49,** 1484–1496.

Oh DH, Leidi E, Zhang Q, *et al*. 2009. Loss of halophytism by interference with SOS1 expression. *Plant Physiology* **151,** 210–222.

Orlowski J, Grinstein S. 2007. Emerging roles of alkali cation/proton exchangers in organellar homeostasis. *Current Opinion in Cell Biology* **19,** 483–492.

Pittman JK, Shigaki T, Hirschi KD. 2005. Evidence of differential pH regulation of the Arabidopsis vacuolar Ca^{2+}/H^+ antiporters CAX1 and CAX2. *FEBS Letters* **579,** 2648–2656.

Qiu QS, Guo Y, Dietrich MA, Schumaker KS, Zhu JK. 2002. Regulation of SOS1, a plasma membrane Na^+/H^+ exchanger in *Arabidopsis thaliana*, by SOS2 and SOS3. *Proceedings of the National Academy of Sciences, USA* **99,** 8436–8441.

Qiu QS, Guo Y, Quintero FJ, Pardo JM, Schumaker KS, Zhu JK. 2004. Regulation of vacuolar Na^+/H^+ exchange in *Arabidopsis thaliana*

by the salt-overly-sensitive (SOS) pathway. *Journal of Biological Chemistry* **279,** 207–215.

Quintero FJ, Ohta M, Shi H, Zhu JK, Pardo JM. 2002. Reconstitution in yeast of the Arabidopsis SOS signaling pathway for Na^+ homeostasis. *Proceedings of the National Academy of Sciences, USA* **99,** 9061–9066.

Reichardt I, Stierhof YD, Mayer U, Richter S, Schwarz H, Schumacher K, Jurgens G. 2007. Plant cytokinesis requires *de novo* secretory trafficking but not endocytosis. *Current Biology* **17,** 2047–2053.

Rus A, Lee BH, Munoz-Mayor A, Sharkhuu A, Miura K, Zhu JK, Bressan RA, Hasegawa PM. 2004. AtHKT1 facilitates Na^+ homeostasis and K^+ nutrition *in planta*. *Plant Physiology* **136,** 2500–2511.

Rus A, Yokoi S, Sharkhuu A, Reddy M, Lee BH, Matsumoto TK, Koiwa H, Zhu JK, Bressan RA, Hasegawa PM. 2001. AtHKT1 is a salt tolerance determinant that controls Na^+ entry into plant roots. *Proceedings of the National Academy of Sciences, USA* **98,** 14150–14155.

Shabala L, Cuin TA, Newman IA, Shabala S. 2005. Salinity-induced ion flux patterns from the excised roots of Arabidopsis *sos* mutants. *Planta* **222,** 1041–1050.

Shi H, Ishitani M, Kim C, Zhu JK. 2000. The *Arabidopsis thaliana* salt tolerance gene *SOS1* encodes a putative Na^+/H^+ antiporter. *Proceedings of the National Academy of Sciences, USA* **97,** 6896–6901.

Shi H, Quintero FJ, Pardo JM, Zhu JK. 2002. The putative plasma membrane Na^+/H^+ antiporter SOS1 controls long-distance Na^+ transport in plants. *The Plant Cell* **14,** 465–477.

Tracy FE, Gilliham M, Dodd AN, Webb AA, Tester M. 2008. NaCl-induced changes in cytosolic free Ca^{2+} in *Arabidopsis thaliana* are heterogeneous and modified by external ionic composition. *Plant, Cell and Environment* **31,** 1063–1073.

Turk M, Mejanelle L, Sentjurc M, Grimalt JO, Gunde-Cimerman N, Plemenitas A. 2004. Salt-induced changes in lipid composition and membrane fluidity of halophilic yeast-like melanized fungi. *Extremophiles* **8,** 53–61.

Turk M, Montiel V, Zigon D, Plemenitas A, Ramos J. 2007. Plasma membrane composition of *Debaryomyces hansenii* adapts to changes in pH and external salinity. *Microbiology* **153,** 3586–3592.

Tyrrell M, Campanoni P, Sutter JU, Pratelli R, Paneque M, Sokolovski S, Blatt MR. 2007. Selective targeting of plasma membrane and tonoplast traffic by inhibitory (dominant-negative) SNARE fragments. *The Plant Journal* **51,** 1099–1115.

Wu SJ, Ding L, Zhu JK. 1996. *SOS1*, a genetic locus essential for salt tolerance and potassium acquisition. *The Plant Cell* **8,** 617–627.

Yamaguchi T, Aharon GS, Sottosanto JB, Blumwald E. 2005. Vacuolar Na^+/H^+ antiporter cation selectivity is regulated by calmodulin from within the vacuole in a Ca^{2+}- and pH-dependent manner. *Proceedings of the National Academy of Sciences, USA* **102,** 16107–16112.

Zhu JK. 2001. Plant salt tolerance. *Trends in Plant Science* **6,** 66–71.